Discovery of Two Nearby Post-T Tauri Stellar Associations

Jiaming Liu[1,5] , Min Fang[2] , and Chao Liu[3,4]
[1] Key Lab of Optical Astronomy, National Astronomical Observatories, CAS, Beijing 100101, People's Republic of China; jmliu@nao.cas.cn
[2] Department of Astronomy, University of Arizona, 933 North Cherry Avenue, Tucson, AZ 85721, USA; mfang@email.arizona.edu
[3] University of Chinese Academy of Sciences, Beijing 100049, People's Republic of China
[4] Key Lab of Space Astronomy and Technology, National Astronomical Observatories, CAS, Beijing 100101, People's Republic of China; liuchao@nao.cas.cn
Received 2019 September 25; revised 2020 January 7; accepted 2020 January 12; published 2020 February 13

Abstract

In this work we report the discovery of two new stellar associations in close vicinity of the Sun at roughly 180 and 150 pc. These two associations, u Tau assoc and e Tau assoc, were detected based on their clustering in a multi-dimensional parameter space including α, δ, μ_α, μ_δ, and ϖ of *Gaia*. The fitting of pre-main-sequence model isochrones in their color–magnitude diagrams suggests that the two associations are of about 50 Myr old and the group members lower than $\sim$0.8 $M_\odot$ are at the stage of post-T Tauri.

Unified Astronomy Thesaurus concepts: Pre-main sequence (1289); Pre-main sequence stars (1290); Young star clusters (1833)

1. Introduction

Stellar associations, as fundamental blocks of our Milky Way, will help us to understand the formation and evolution of the structures of the Milky Way. Nearby young associations are particularly important, and are excellent laboratories for studying the initial mass functions (IMF) in the extremely low-mass range (Gagné et al. 2018) and the formation and early evolution of planetary systems and brown dwarfs (BD; Chauvin et al. 2015), since young objects of substellar and planetary mass range are comparatively bright and easily detected. However, due to the low stellar density and large extension in the sky, nearby young associations and their members are hard to identified. Members of them are newly formed in same molecular cloud and have not been significantly perturbed by the Galaxy, thus they usually share some common properties such as age, chemical composition, distance, and kinematics (Song et al. 2003; Torres et al. 2008; Gagné et al. 2018). Therefore, these stars will usually show significant concentration in multi-dimensional astrometric space and be identified as overdensities from its surrounding field stars (Fürnkranz et al. 2019).

Recently, *Gaia* DR2 data, which provide position and *G*-band (330–1050 nm) photometric data down to a magnitude 21 for 1.7 billion stars, including parallax and proper motions for over 1.3 billion stars and radial velocities for stars brighter than 13 magnitude in the *G* band (Gaia Collaboration et al. 2016, 2017, 2018), will definitely promote the membership completeness of current stellar associations and boost the discovery of new stellar associations. Here, we report the discovery of two new young associations near Taurus.

This work is arranged as follows. In Section 2, we describe the data and refine the membership of the associations. The population properties will be discussed in Section 3 followed by a brief discussion in Section 4, and finally summary and conclusions in Section 5.

2. Data and Membership

2.1. Data Selection

During a study about the young stellar associations of Taurus (J. Liu et al. 2020, in preparation) with *Gaia* DR2 data, we notice that apart from those known associations, there are two likely stellar associations near Taurus, located at roughly 150 and 180 pc that have not been realized before. The two candidates of the associations that are roughly centered to (+21.21, −13.94) and (+24.22, −24.02) of (μ_α, μ_δ) are clearly notable from their surrounding field stars as outstanding overdensities in the proper motion space (see Figure 1). Stars employed in this plot are selected by 50°–65° of α, 0°–20° of δ, 15–35 mas yr^{-1} of μ_α, −30 to −5 mas yr^{-1} of μ_δ, and 100–200 pc of distance. As the two associations are tightly clustered in the proper motion space, to refine their memberships, the data we selected are based on the following criteria: (1) all of the sources around the center of these two associations have a radius of 5 mas yr^{-1} from the proper motion space, slightly larger than the radii of the associations; (2) a parallax quality of $\sigma_\varpi/\varpi \leqslant 0.1$; (3) the flux error of G_{RP} is smaller than 5%, considering that the typical distance extension for nearby young associations is usually $\sim$20 pc (Gagné et al. 2018); thus (4) the distance cut is set to be 100–200 pc from the Sun. In total we have 448 stars.

2.2. Membership

Membership refinement by their concentration in multiple astrometric space is the most commonly used method for associations showing clear overdensities in the astrometric space. Considering members of the nearby associations are usually loosely concentrated in the spatial space, a friend-of-friends (FOF) algorithm of ROCKSTAR[6] is adopted (Behroozi

---

[6] ROCKSTAR is based on the adaptive hierarchical refinement of friends-of-friends (FOF) groups in six phase-space dimensions, which allows for the tracking of a high number density clusters, and divided all the stars into several groups excluding those stars that could not be vested in the star aggregates. It is designed to find outlier structures that tightly connect in the 6D space, as *Gaia* DR2 only provides the radial velocity for bright stars with *G*-band magnitude brighter than 13.0. Thus, to adopt ROCKSTAR, we set the radial velocity as zero for all sample stars and keep the other 5D coordinates as α, δ, μ_α, and μ_δ, and distances as given by Bailer-Jones et al. (2018).
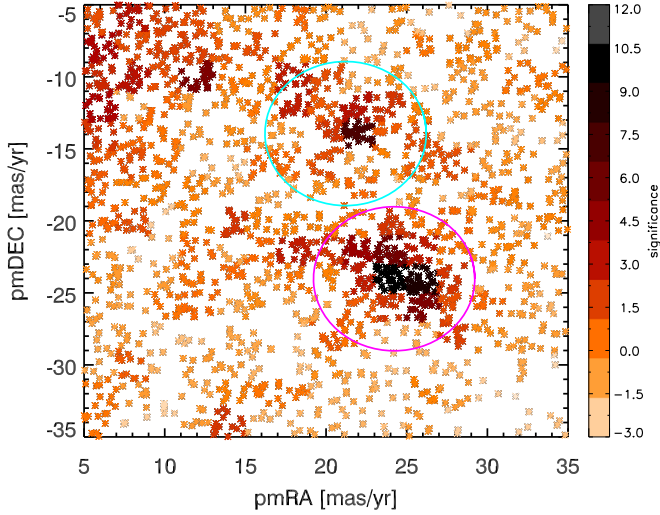
Figure 1. Location of the two associations in μ_α, μ_δ space. Based on their locations in the proper motion, the stars are divided into a series of bins of $2\,\mathrm{mas\,yr^{-1}} \times 2\,\mathrm{mas\,yr^{-1}}$, while the colors of the symbols in each bin denote the significance of them. Cyan and purple circles are the $5\,\mathrm{mas\,yr^{-1}}$ region around the center of the potential associations.

Figure 2. Location of the two associations at α, δ space (lower left panel), μ_α, μ_δ space (upper left panel), and the distance distribution (right panel). The background contour in the lower left panel is the 350 μm dust emission map of Planck.

et al. 2013). Based on the sample stars input, ROCKSTAR will automatically modify the linking space between members of friend stars, divide them into several groups, and label those isolated individual stars out. Thus, with these 448 stars we selected above, we ruled out the surrounding field stars by eliminating isolated stars at each run time. After three iterations of ROCKSTAR, the stars left are spatially concentrated in two groups (see Figure 2), which contain 35 and 119 members, respectively. We regard them as u Tau assoc and e Tau assoc (see Tables 1 and 2 for detailed information) hereafter. A reliability test of ROCKSTAR in refining memberships of the two associations is proven in the Appendix. ROCKSTAR can find out ∼95% of the group members at a purity level of ∼90%, proving that the ROCKSTAR method is an effective way to refine the memberships of the Tau assocs kind. Figure 2 shows the locations of the associations, the cyan asterisks indicate the stars of u Tau assoc, and the purple crosses represent the members of e Tau assoc. The association u Tau assoc, located at roughly 180 pc from the Sun, is tightly concentrated in both α and δ (centered at $56°.0$, $5°.46$) and proper motion space. The e Tau assoc is located at 150 pc from the Sun, tightly concentrated in the proper motion space but largely extended in the α and δ space (centered at $57°.69$, $10°.16$).

2.3. Spectra Data

The spectra data adapted in this work are taken from Large Sky Area Multi-Object Fibre Spectroscopic Telescope (LAMOST). LAMOST is a 4 m Schmidt telescope of the National Astronomical Observatories, located at Xinglong Observing Station, China. With 4000 fibers on board the focus, LAMOST can observe nearly 4000 optical spectra in 20 square degrees at a time (Cui et al. 2012). Since 2012, LAMOST has released its surveying data seven times. The data engaged in this work are taken from the recently released data DR5. LAMOST DR5 provides over nine million spectra as well as a catalog of general stellar parameters derived from the spectra for over five million stars. With the LAMOST data, we will discuss some properties of the associations later.
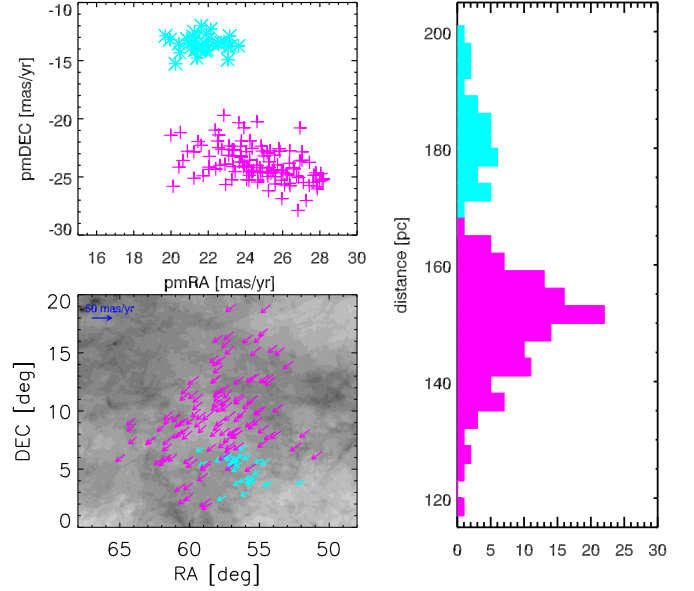
3. Population Properties

3.1. Convergent Point (CP)

As a projection effect, the co-moving members of an association usually converge to a certain point of the celestial sphere, known as CP (Galli et al. 2012). The CP point, ever since its first presented by Bohlin in 1916 (Smart 1968), has also been used as an important tool for testing membership of associations. Since then a lot of different methods have been introduced for its solution (Jones 1971; de Bruijne 1999; Galli et al. 2012). In order to confirm that these two new associations are not from the same group, we derive their CPs of the equatorial coordinates. The CPs for u Tau assoc and e Tau assoc are $(98°.06,\ -19°.32) \pm (0°.67,\ 0°.36)$ and $(108°.39,\ -33°.23) \pm (0°.54,\ 0°.28)$, respectively. The difference of the CPs is evident that the two associations, although close in location and share similar properties, are indeed two separate ones.

3.2. Age and Mass

Figure 3 shows the color–magnitude diagrams (CMDs) for the two associations. The gray dots are the foreground stars in the same direction but within 100 pc from the Sun, and are regarded as main-sequence (MS) stars here. The foreground stars are selected based on the following criteria: (1) the stars are in the region of $0°$–$20°$ of α and $50°$–$65°$ of δ; (2) $\sigma_\varpi/\varpi \leqslant 0.1$; (3) the flux error of G_{RP} is smaller than 5%; and (4) the stars are within 100 pc from the Sun. In total we have 1934 stars. Asterisks and crosses represent for the members of the associations u Tau assoc and e Tau assoc, respectively. Interstellar extinction is corrected using the Galactic average extinction law of $R_V = 3.1$, where $R_V = A_V/E(B - V)$ is the total to selective coefficient. Since the V-band interstellar extinction is about 0.7–$1.0\,\mathrm{mag\,kpc^{-1}}$ in the solar neighborhood (Gottlieb & Upson 1969; Milne & Aller 1980; Wang et al. 2017), a mean value of $0.85\,\mathrm{mag\,kpc^{-1}}$ is taken here. Then for each individual star at distance D, its V-band

Table 1
Members of u Tau assoc

Gaia ID	Other Names	RAJ2000 (deg)	DEJ2000 (deg)	pmRA (mas yr^{-1})	pmDEC (mas yr^{-1})	Distance (pc)	R_V (km s^{-1})	Spectral Type
3275316947256508160		51.736	4.043	21.629	−12.003	169.957		
3274385076792329600		54.059	3.927	23.147	−12.892	190.228		
3274390707494059008	TYC 67-1230-1	54.099	3.927	23.626	−13.737	171.170	17.960	
3275975863959274752		54.276	5.830	23.058	−14.917	185.967		
3275991188402579584		54.725	5.894	22.249	−13.610	180.059		
3275104191756729728		54.853	4.913	22.005	−13.117	192.334		
3274743551942762624	HD 22903	55.202	4.317	21.904	−12.699	179.276		A1V
3274716064152131584		55.248	3.977	23.079	−13.807	173.449		
3274845153689271552		55.338	4.515	22.543	−13.525	175.622		
3274725994116512128		55.358	4.169	22.856	−13.424	172.744		
3276764076357778944		55.542	6.225	21.869	−14.103	178.589		
3271397600621973120		55.752	3.056	21.255	−12.536	185.012		
3277675674577524736		55.892	7.032	21.395	−14.778	182.235		
3271821286258516608	HD 23248	55.916	4.213	21.191	−12.935	181.532		A5II/II
3276862310851856512	TYC 71-674-1	55.954	6.369	21.940	−14.034	180.029	16.700	
3276494111894881536		56.166	5.625	21.650	−13.876	176.280		
3271752777237464960	V* V1273 Tau	56.222	3.992	22.694	−13.444	173.999	12.480	K2
3276798401738487808		56.288	6.201	21.826	−14.176	176.509		
3276386050517837696		56.402	5.186	20.473	−14.314	187.407		
3276605295710700032	* u Tau	56.419	6.050	21.878	−13.646	187.893		B3V
3276604544094119424		56.421	6.043	21.272	−14.111	182.324		
3276604544093968896		56.428	6.051	21.108	−13.801	179.229		
3276604922051089664		56.435	6.058	19.950	−13.189	178.949	15.820	G9
3276490121867896448		56.441	5.734	22.133	−12.300	196.321	17.220	G8
3276586333432639744		56.523	5.885	21.409	−13.928	178.837		
3276584478006772224		56.531	5.803	21.416	−14.028	173.695		
3276527406481433600		56.745	5.569	21.463	−13.828	185.585		
3276620315213926400		56.878	6.125	21.276	−13.085	197.202		
3276641446452946304		56.959	6.297	20.959	−13.265	183.644		
3276629386183056768	TYC 71-542-1	56.987	6.269	21.191	−13.396	184.213	16.630	G2
3276624227927031296		57.131	6.178	20.870	−13.151	187.155		
3270622066967091840		57.343	2.706	23.208	−13.737	167.057	16.930	K5
3276932847096564736		57.601	6.041	20.242	−15.262	177.833		
3273682832461023232	BD+05 560	58.771	5.680	20.421	−13.529	200.909		A5
3274101952549519232		58.980	6.854	19.703	−12.866	194.851		

extinction A_V should be $0.85 \times D$. Finally, with the extinction coefficient for *Gaia*, G_{BP} and G_{RP} bands of $R_V = 3.1$ provided by Wang & Chen (2019), the G_{BP} and G_{RP} extinction for each individual star of both foreground MS stars, and the associations members are corrected. The mean *V*-band extinctions for u Tau assoc and e Tau assoc are 0.154 mag and 0.127 mag, respectively.

The blue dashed line in each panel is the best-fit isochrone of stellar tracks and isochrones with the PAdova and TRieste Stellar Evolution Code (PARSEC; Bressan et al. 2012) of solar metallicity. The fit is done as follows: for each isochrone of a certain age, stars within the color and absolute magnitude range of the isochrone are selected. Distances of an isochrone to each of these stars are derived, as the number of stars inside the color and magnitude range is different from isochrone to isochrone, thus the isochrones with the smallest mean distance to the stars are regarded as the best fit. The result showed that these two associations are both young, 50 Myr for u Tau assoc and 46 Myr for e Tau assoc. Actually, as a result of core fusion and convection, surface lithium abundance will deplete with time, and can also be used to estimate age of pre-main-sequence (PMS) stars (Herbig 1965; Weymann & Sears 1965). But this method is not appropriate for LAMOST low-resolution spectra, whose resolution is ~1800 and from which it is hard to deduce

the lithium abundance accurately. Therefore an Li-based method is not considered in this work.

In order to better confirm the results of the age estimation, we alternatively considered the semi-empirical PMS model isochrones of Bell et al. (2014) for Sloan Digital Sky Survey (SDSS) bands, which they derived base on the Pisa PMS isochrones of Tognelli et al. (2012). Realizing that over half of the stars lack SDSS observations, thus we cross-match the members of Tau assocs to the Panoramic Survey Telescope and Rapid Response System (Pan-STARRS; Chambers et al. 2016), of which only two stars of e Tau assoc have no counterparts. But to control the security of the model fit, only those stars with good-quality measurements of PanSTARRS (quality flags of 4, 8, and 16) are conserved (32 stars of u Tau assoc and 106 stars of e Tau assoc). Then we transferred these photometric data of PanSTARRS to SDSS bands with the method of Tonry et al. (2012), of which the transition accuracy is better than 0.002 and 0.003 mag in the *r* and *i* bands, respectively. The model fit result is also shown in Figure 3, and the ages are estimated to be 58 and 54 Myr for u Tau assoc and e Tau assoc, respectively, which agree with the age estimation of PARSEC.

Besides, the transition point (e.g., the turn-on point, TOn) from PMS to MS can also be used to estimate the age of young stellar groups, as the TOn point on the CMD will become

Table 2
Members of e Tau assoc

Gaia ID	Other Names	RAJ2000 (deg)	DEJ2000 (deg)	pmRA (mas yr^{-1})	pmDEC (mas yr^{-1})	Distance (pc)	R_V (km s^{-1})	Spectral Type
9509336766831744		50.505	6.508	26.382	−22.743	133.808		
10942515813999488	HD 21194	51.362	8.427	26.855	−25.050	136.770	19.460	F5
99936716391 20256	BD+06 533	51.991	7.255	27.982	−25.361	134.707		F8
41872327659525504		52.540	14.325	26.191	−24.738	148.766		
42352367565698304		53.199	15.473	24.905	−24.567	150.619		
13078626388631424	V* V1267 Tau	53.298	10.599	26.370	−25.552	136.872	15.080	K3
11397988505713536	HD 22073	53.444	8.291	27.040	−23.569	146.711		A5
42440500294245120		53.754	15.662	22.055	−23.234	156.706		
11472617857575552		53.869	8.199	27.438	−23.753	142.724		
40695158727074048		53.895	12.884	24.773	−24.208	163.725		
40705848902910464		54.027	13.128	27.849	−25.848	144.380		
57153099745350912		54.208	19.135	24.200	−24.869	150.991		
40726224227818240		54.306	13.125	25.209	−24.951	156.096		
11522435182853120		54.325	8.793	27.684	−24.865	142.689		
3277897741565006976		54.382	7.551	25.466	−24.476	145.419		
44258027374647808		54.396	17.088	23.681	−23.716	158.050	12.740	K7
12343637226131584	TYC 660-709-1	54.576	10.338	26.748	−24.923	146.051	14.560	G9
12355628774864128		54.704	10.363	25.724	−23.969	147.480		
44034311118104320		54.718	16.595	22.937	−25.649	158.159		
11959323551830912		54.793	9.466	24.434	−24.441	144.029	17.040	K3
41651772500169984	TYC 1235-156-1	54.915	15.499	25.957	−26.861	155.433	15.870	
38088873789758720	BD+12 500	55.042	13.199	25.527	−24.403	150.120	14.170	F8
11888473771374848		55.143	9.114	23.332	−24.108	147.665		
37195348793250048		55.154	11.293	27.113	−25.476	142.693		
38076641722829440	TYC 663-362-1	55.241	13.151	24.656	−25.443	147.577	13.360	
3275164390018316288		55.273	5.454	26.928	−23.628	141.578		
11985196435903488		55.283	9.285	24.988	−23.192	149.482		
36420502331404160	TYC 660-135-1	55.442	10.908	26.399	−25.756	140.121	14.500	
44057778819482496		55.515	16.528	24.365	−24.625	150.486		
36103396308075776		55.966	10.088	22.041	−24.349	150.297		
36530487856056704		56.072	11.303	26.253	−24.827	136.375		
3277686910210391296	2MASS J03442859+0716	56.119	7.270	25.801	−22.564	150.709		M4
36537737760831744		56.126	11.501	25.259	−24.176	149.959		
37844713488859264		56.147	12.959	24.614	−24.007	154.850		
36034023996411392		56.179	9.738	22.636	−24.009	150.274		
3278197770802258944	HD 23376	56.246	8.320	26.612	−24.306	144.644	16.490	G5
3278197766505583232	TYC 658-1007-2	56.246	8.321	26.577	−24.198	142.418	20.640	
3278487145518773248		56.306	8.616	26.363	−23.826	155.014		
3278300987456845440	TYC 658-828-1	56.467	8.541	27.783	−24.644	131.926	15.590	
3278489313182286720		56.501	8.609	27.791	−24.834	135.925		
50970717660507008		56.690	19.189	25.563	−23.138	154.909		
3272287615693093376		56.717	7.078	27.049	−22.842	150.719		
3273313144978675840		56.726	7.344	25.167	−22.944	142.686		
3302676747927557504		56.741	9.945	27.262	−27.025	137.566		
3276420135378285056		56.798	5.440	22.837	−19.710	163.312		
42956995881088256		56.847	15.557	21.727	−24.897	157.735		
43660752042391680		56.849	16.808	24.806	−24.601	154.295		
3278204402232390528	BD+07 543	56.880	7.957	25.369	−24.690	155.451	14.640	F8
36203417507399808		56.966	10.724	27.642	−25.464	158.885		
36901298152686080	TYC 661-560-1	56.974	11.816	21.230	−25.115	154.141	15.450	
43059486684334208		57.043	16.145	23.268	−25.243	159.908		
36290072767519232	* e Tau	57.068	11.143	25.269	−23.695	128.770		B3V
36290107127257344	TYC 661-1404-1	57.070	11.145	25.616	−24.972	137.914	19.560	F3Vn
3278259858850059264	TYC 658-922-1	57.131	8.527	25.327	−22.738	151.878	8.520	G7
36941189808895872		57.184	12.220	23.753	−23.215	159.044	11.880	K7
3276628183593979904		57.218	6.342	23.643	−20.334	155.848		
3277330153049126400		57.228	7.465	24.847	−22.347	150.250		
3302817966452511616		57.425	10.591	24.606	−24.003	149.917		
3302396166303947904	HD 23990	57.444	9.407	25.165	−24.660	147.495		B9
39846683645349376		57.460	14.682	22.024	−24.158	154.757		
36924353537157632		57.522	12.071	24.224	−23.552	153.293		
36701702432783616		57.572	11.496	24.337	−24.516	150.262		
43458167025621504	2MASS J03502840+1631	57.618	16.521	24.242	−21.892	146.359	7.390	G5IV

4

Table 2
(Continued)

Gaia ID	Other Names	RAJ2000 (deg)	DEJ2000 (deg)	pmRA (mas yr^{-1})	pmDEC (mas yr^{-1})	Distance (pc)	R_V (km s^{-1})	Spectral Type
39513359823463680		57.620	13.937	23.942	−24.043	149.477		
3302299134402909056		57.638	8.930	24.037	−22.827	154.236		
367246203782489984		57.683	11.809	22.542	−22.481	165.514		
36595943156045824	BD+10 496	57.711	11.002	24.137	−24.167	151.392	14.960	F8
3302822811175649664		57.724	10.702	26.015	−24.606	141.009		
39641487287397632		57.772	14.526	20.639	−23.587	154.918		
3301516179044339840		57.786	8.489	25.935	−24.427	137.591		
37136524921755904		57.793	13.046	23.101	−23.138	162.124		
37136834159399808	V* V766 Tau	57.816	13.046	23.769	−23.228	160.771		B9pSi
39841357885932288	TYC 664-136-1	57.915	14.797	23.833	−23.721	159.686	28.720	
3277156567650183680		58.149	7.156	21.228	−22.856	158.009		
3270343546928113664	HD 24456	58.376	2.119	26.933	−20.785	138.680		B9V
3273850404904742912	TYC 72-816-1	58.449	5.707	28.184	−25.182	132.266	27.560	
3270377941026192768		58.506	2.484	26.104	−25.683	124.607		
3273648919399332608	TYC 72-620-1	58.513	5.431	24.625	−20.253	142.703	22.210	
3273169120012500736		58.707	4.624	25.847	−22.798	141.751		
3301633517550972032		58.811	8.800	20.422	−24.161	154.244		
3302850402044815104		58.836	9.921	23.750	−23.323	151.633		
3301687599779043584		58.933	9.301	25.201	−24.605	149.626		
3303308245556503296	HD 286374	59.080	11.420	24.048	−24.124	152.306	13.600	F5
3303061851874905088	HD 286380	59.086	10.797	24.658	−25.252	147.681	14.650	G5
3302885135443350144		59.206	10.174	23.899	−24.142	150.217		
38398936068862464	TYC 665-150-1	59.339	12.971	28.046	−24.709	152.421		G0
3303319927869595264		59.412	11.709	23.298	−23.208	154.757		
3273771824183136256		59.428	5.856	28.109	−25.250	126.075		
3302063667115147008	2MASS J03581272+0932	59.553	9.540	24.321	−24.493	146.782	16.120	K3
3273802232551662336		59.748	6.092	24.363	−22.545	150.096		
3272119941104628352		59.750	3.837	23.782	−21.905	156.004		
3259900660364779392		59.767	2.881	21.447	−21.952	142.016		
3301312838112630400		59.814	8.289	25.603	−25.603	149.855		
3304906145189468416	TYC 662-217-1	59.926	12.169	24.066	−25.242	148.495	15.290	
3304619413175027968		60.004	11.611	24.188	−25.297	146.915		
3301396126118384768		60.013	8.653	23.291	−22.675	158.536		
3259830325980399744		60.132	2.593	23.916	−20.774	152.736		
3302018999455336192		60.158	9.367	22.724	−22.632	157.019		
3301329949262394624		60.292	8.406	23.114	−22.334	152.465		
3301831773241303552	BD+08 616	60.339	9.334	25.238	−26.184	155.343	42.580	F8
3272433615452990848		60.347	3.709	24.897	−22.773	140.743		
3298319348986238464		60.553	8.294	23.378	−22.681	150.586		
3301945366536236416		60.698	9.776	20.112	−25.812	146.839		
3297800516936921344		60.738	6.383	27.282	−26.218	135.379	−35.940	
3297045667844723712		60.893	6.298	23.739	−22.357	142.644		
3298606905637432576		61.165	7.866	26.820	−27.881	158.535		
3301900595797205632		61.206	9.585	22.404	−24.313	150.938		
3301974331795653888		61.211	9.936	22.900	−23.903	150.802		
3297959396367266560		61.304	7.172	22.500	−21.909	157.938		
3297032886022084864		61.344	6.259	23.325	−22.646	153.044		
3296973134437145984		61.436	6.014	27.429	−25.740	161.976		
3298826700586330240		61.667	8.941	23.444	−24.541	138.867		
3297062675915933696		61.753	6.119	27.861	−26.029	119.267		
3298371507070141056	TYC 666-80-1	62.448	7.801	21.622	−22.284	157.801	19.060	
3297619097518627968	HD 26323	62.529	7.698	22.376	−20.975	161.069		B9
3297662204719373440		63.798	7.764	20.502	−21.183	163.552		
3293306676067811200	* mu. Tau	63.884	8.892	20.881	−22.789	149.992		B3IV
3300180959610801536		63.944	9.357	19.986	−21.413	163.528		
3285243784909511168		64.650	6.244	22.561	−21.392	159.112		

flatter and drop to the MS tracks as the stellar group grows old (Cignoni et al. 2010). Therefore, TOn can also serve as an indicator of the age for clusters that are sufficiently young and contain PMS members. In light of this, the TOn of the PARSEC model is also considered as a validation of our age estimation. The result of this approach is shown in Figure 4. TOns of the Tau assocs are both consistent with that of 50 Myr, with the TOn point roughly corresponding to a ∼0.8$M_\odot$ star.

With the best-fit isochrones of PARSEC, the stellar masses are then estimated. The mass range of the associations
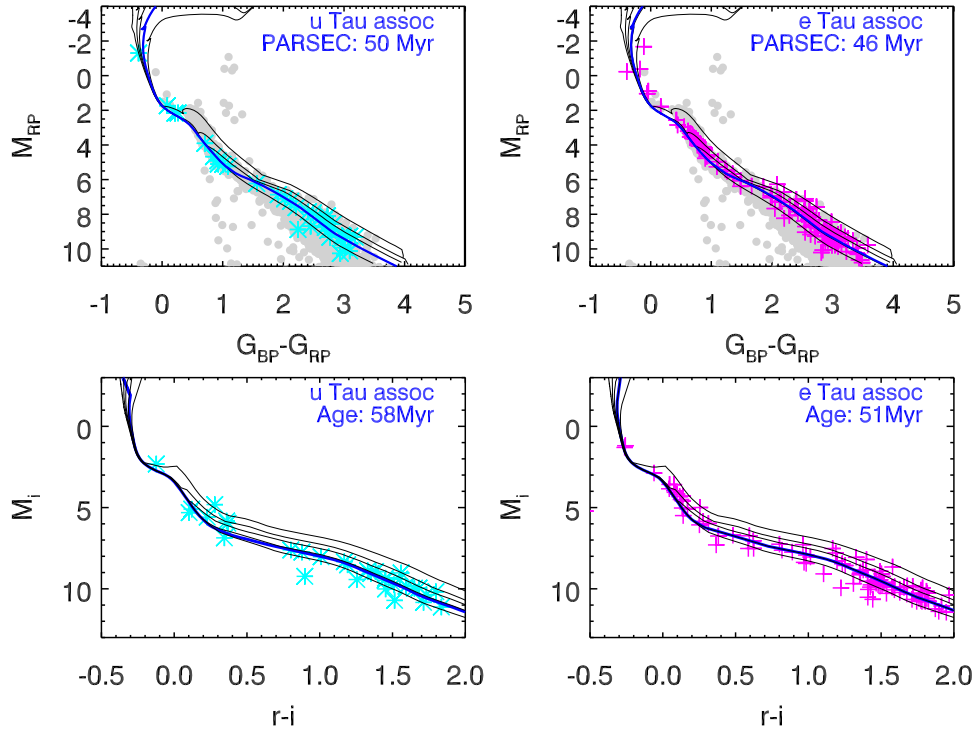
Figure 3. Color–magnitude diagram of Tau assocs. Gray dots are the foreground main-sequence stars in the same direction. Cyan asterisks denote the u Tau assoc, while purple crosses indicate members of e Tau assoc. The blue solid lines are the best-fit isochrones of PARSEC (upper panels) and the model of Bell et al. (2014, lower panels). The thin black lines from top to bottom in each panel denote isochrones of 10, 20, 30, 50, and 100 Myr.
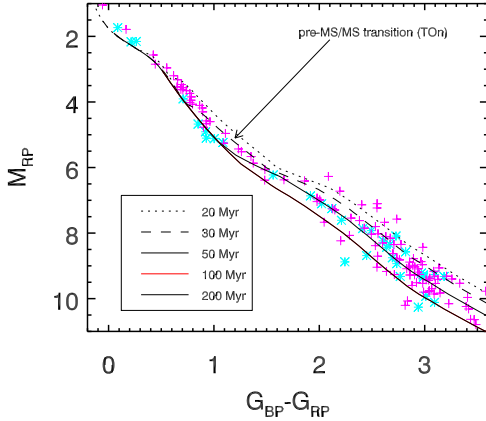

Figure 4. Pre-main-sequence tracks of different ages given by PARSEC. Also plotted are the members of the Tau assocs with symbols defined the same as the previous figures.

Figure 5. Mass estimation of the associations based on the IMF model of Kroupa (2001).

demonstrate that most of their members have low mass (subsolar mass) with a few of them having masses larger than solar mass, and an upper limit of $\sim 6.0 M_\odot$. Based on the masses of the stars, we fit the present-day mass functions to a series of IMF of Kroupa (2001), and the total mass of the two associations are estimated to be ~ 40 and ~ 160 $M_\odot$, respectively, for u Tau assoc and e Tau assoc (see Figure 5).

3.3. Radial Velocity and Metallicity

Radial velocity is an important parameter of kinematics, especially for the stars of the associations. Since *Gaia* DR2 only provided the radial velocities for bright stars, 7 stars in u Tau assoc and 29 in e Tau assoc have *Gaia* released radial velocities. We also searched members of the associations in the LAMOST DR5, and of them 23 stars are found, but only one is

new. In a word, we have 8 members of u Tau assoc and 29 members of e Tau assoc with radial velocity information. The histograms of the radial velocity for the associations are plotted in Figure 6. A rough examination showed that the mean value of the radial velocity of u Tau assoc is $16 \, \mathrm{km \, s^{-1}}$ with a dispersion of $2 \, \mathrm{km \, s^{-1}}$, while for e Tau assoc the average value is $15 \, \mathrm{km \, s^{-1}}$ and a dispersion of $5 \, \mathrm{km \, s^{-1}}$.

Besides radial velocity, LAMOST DR5 also provided metallicities for 7 stars in u Tau assoc and 16 in e Tau assoc. The mean metallicity for u Tau assoc and e Tau assoc are 0.03 and 0.03 dex, respectively.

4. Discussion

Associations, especially nearby associations, are the ideal laboratory for studying stellar kinematics and the evolution of
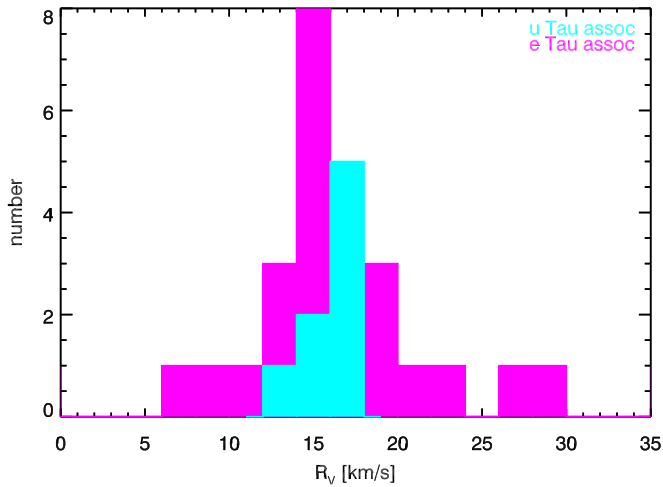
Figure 6. Radial velocity histogram of Tau assocs. Cyan represents the u Tau assoc and purple represents the e Tau assoc.

Figure 7. Hα equivalent width of Tau assocs members (cyan asterisks for u Tau assoc and purple crosses for e Tau assoc) compared with those of known Taurus PMS stars with no disk (Esplin et al. 2014, shown as open black circles).

stars in groups, and therefore, efforts have been taken to search for more new associations, especially after the data release of *Gaia*. Quite soon after the first data release of *Gaia*, Oh et al. (2017) applied a marginalized-likelihood ratio test to the Tycho-*Gaia* Astrometric Solution (TGAS), searching for co-moving pairs from field stars. From 10,606 unique stars, by a connection radius of 10 pc, they find 13,085 co-moving star pairs. Later, Faherty et al. (2018) pushed the work forward and reexamined the result of Oh et al. (2017) with the bayesian method BANYAN Σ, and apart from those associations of already known, they also reported over 20 potential new stellar groups. Among their potential stars in the groups, 10 members of the association e Tau assoc of this work are included, but were separated in three different groups. A likely reason for this is that at the time of their work, TGAS was short in stars, and as e Tau assoc is largely extended in the space, it is natural that the members were not linked together and divided into several parts. On the other hand, their work also confirmed the fact that these stars are clustered in groups.

A 2″ radius cross-match with SIMBAD shows that these two associations in total contain 43 counterparts, including 3 B3, 4 B9, 1 A1, 3 A5, 8 F type, 7 G type, 3 K type, and 1 M type stars (13 with no spectra type information). This is consistent with the mass estimation results in Section 3.2 that the associations of this work contain a few stars of several solar masses. Tetzlaff et al. (2011) published a catalog of young *Hipparcos* stars within 3 kpc from the Sun. Four of the 43 SIMBAD sources in this work are included, and the ages are estimated as 5.7, 7.0, 13.4s and 37.8 Myr, which are younger than the ages of this work. The difference is understandable since both works use different distances. In Tetzlaff et al. (2011), they adopted the distances from *Hipparcos*, and with seven sets of evolutionary models, they derived the median ages from them (see Tetzlaff et al. 2011 for details). For two sources with ages of 5.7 or 7.0 Myr in Tetzlaff et al. (2011), there are large differences between the distances from *Hipparcos* and *Gaia* with the distances from *Hipparcos* being 26% and 16%, respectively, larger than those from *Gaia*. This can result in higher luminosity and younger ages in Tetzlaff et al. (2011) than in this work. Furthermore, the age of each association in this work is estimated as a whole from the CMD or the TOn, which should provide a better age estimation than just using individual stars.
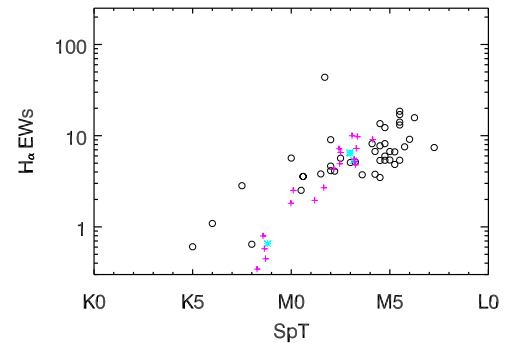
Early in 1978, Herbig introduced post-T Tauri stars (PTTS) in order to explain the lack of older PMS T Tauri stars with ages older than 5–10 Myr in star-forming regions (Herbig 1978). As the distinct characteristics of T Tauri stars, e.g., strong Hα emission, high surface lithium abundance, irregular variability, and color excess of infrared as well as X-ray emission (Walter 1986), are absent at the stage of zero-age main sequence (ZAMS), he argued that the PTTS should show an intermediate or moderate value of these characteristics. Jensen (2001) thought that PTTS are stars older than T Tauri but have not reached ZAMS, and discussed the properties of them in his work. He stated that to certify the validity of PTTS, apart from age estimation, the validity of PTTS should be further confirmed by at least one or two characteristics of T Tauri stars.

As the age of the Tau assocs are estimated to be 50 Myr, stars under the TOn ($\sim 0.8 M_\odot$) should be post-T Tauri stars. To certify the validity, spectra of the Tau assocs observed by LAMOST are examined. In total 44 of them have been observed, their equivalent width of the Hα line confirmed that the transition from absorption to emission is roughly around the TOn, and the 18 stars with a mass lower than the TOn mass do obviously show an Hα emission feature. Comparing their Hα equivalent width to that of previously known T Tauri stars with no circumstellar disk (Esplin et al. 2014), it shows that the intensities are comparatively moderate to that of T Tauri stars (see Figure 7), manifesting their young properties.

5. Summary and Conclusions

In this work, with *Gaia* DR2 astrometric data, by searching the overdensities of nearby stars in the multiphase space, we find two new young stellar associations, u Tau assoc and e Tau assoc, that have not been noticed before. The two associations are quite close to each other, but could be clearly separated. Members of u Tau assoc are tightly concentrated in both α, δ and μ_α, μ_δ space, while the members of e Tau assoc, although also concentrated in the proper motion space, are more extended in the α and δ space within nearly 200 square degrees. These two associations are of solar metallicity and are young, with their best-fit isochrone ages of about 50 Myr. From the fitting of the PMS model isochrones, the transition from PMS to MS can be identified at $\sim 0.8 M_\odot$, and members lower than $\sim 0.8 M_\odot$ are at the stage of post-T Tauri.
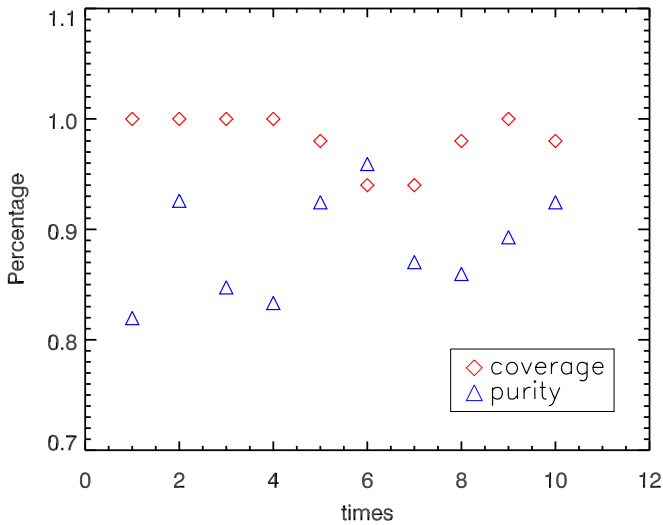
Figure 8. Result of the search for the created association. Coverage means how many of the 50 group stars are located in the result. Purity is the group members left of total number of stars in the process.

Appendix
Reliability Test of ROCKSTAR

The purpose of ROCKSTAR we employed in this work is to refine the memberships and eliminate contaminations of the associations rather than discover associations, since we knew that the two associations are clearly visible in the proper motion space. In considering that the ROCKSTAR code is not originally designed to handle associations, therefore, a test about the effectiveness of ROCKSTAR is necessary. Given that young associations will be questioned about the completeness and contamination, a man-made artificial testing association will be much better. Thus, we randomly created a testing group of 50 stars of the same general properties of Tau assocs (u Tau assoc and e Tau assoc) and a larger region of field stars surround them, also with properties like those of field stars around Tau assocs. With the same selecting criteria used as for the search for them, ROCKSTAR was run three times. We repeated this procedure 10 times, and show the result in Figure 8.

The result shows that in 10 times of testing, ROCKSTAR can find out ∼95% of the group members at a purity level of ∼90%, proving that the code is an effective way to refine the memberships of associations like Tau assocs. By this we mean that the ROCKSTAR code is an effective way to search for members with a likeness of Tau assocs, but not for all associations.

ORCID iDs

Jiaming Liu ⊙ https://orcid.org/0000-0002-4828-0326
Min Fang ⊙ https://orcid.org/0000-0001-8060-1321
Chao Liu ⊙ https://orcid.org/0000-0002-1802-6917

References

Bailer-Jones, C. A. L., Rybizki, J., Fouesneau, M., Mantelet, G., & Andrae, R. 2018, AJ, 156, 58
Behroozi, P. S., Wechsler, R. H., & Wu, H.-Y. 2013, ApJ, 762, 109
Bell, C. P. M., Rees, J. M., Naylor, T., et al. 2014, MNRAS, 445, 3496
Bressan, A., Marigo, P., Girardi, L., et al. 2012, MNRAS, 427, 127
Briceño, C., Calvet, N., Kenyon, S., & Hartmann, L. 1999, AJ, 118, 1354
Briceño, C., Hartmann, L., Stauffer, J., & Martín, E. 1998, AJ, 115, 2074
Briceño, C., Luhman, K. L., Hartmann, L., Stauffer, J. R., & Kirkpatrick, J. D. 2002, ApJ, 580, 317
Cardelli, J. A., Clayton, G. C., & Mathis, J. S. 1989, ApJ, 345, 245
Chambers, K. C., Magnier, E. A., Metcalfe, N., et al. 2016, arXiv:1612.05560
Chauvin, G., Vigan, A., Bonnefoy, M., et al. 2015, A&A, 573, A127
Cignoni, M., Tosi, M., Sabbi, E., et al. 2010, ApJL, 712, L63
Cui, X.-Q., Zhao, Y. H., Chu, Y. Q., et al. 2012, RAA, 12, 1197
de Bruijne, J. H. J. 1999, MNRAS, 306, 381
Dotter, A., Chaboyer, B., Jevremović, D., et al. 2008, ApJS, 178, 89
Esplin, T. L., & Luhman, K. L. 2017, AJ, 154, 134
Esplin, T. L., Luhman, K. L., Faherty, J. K., Mamajek, E. E., & Bochanski, J. J. 2017, AJ, 154, 46
Esplin, T. L., Luhman, K. L., & Mamajek, E. E. 2014, ApJ, 784, 126
Faherty, J. K., Bochanski, J. J., Gagné, J., et al. 2018, ApJ, 863, 91
Fang, M., Kim, J. S., Pascucci, I., et al. 2017, AJ, 153, 188
Feiden, G. A., Jones, J., & Chaboyer, B. 2015, in 18th Cambridge Workshop on Cool Stars, Stellar Systems, and the Sun, ed. G. van Belle & H. C. Harris (Flagstaff, AZ: Lowell Observatory), 171
Fürnkranz, V., Meingast, S., & Alves, J. 2019, A&A, 624, L11
Gagné, J., Mamajek, E. E., Malo, L., et al. 2018, ApJ, 856, 23
Gaia Collaboration, Brown, A. G. A., Vallenari, A., et al. 2016, A&A, 595, A2
Gaia Collaboration, Brown, A. G. A., Vallenari, A., et al. 2018, A&A, 616, A1
Gaia Collaboration, van Leeuwen, F., Vallenari, A., et al. 2017, A&A, 601, A19
Galli, P. A. B., Loinard, L., Ortiz-Léon, G. N., et al. 2018, ApJ, 859, 33
Galli, P. A. B., Teixeira, R., Ducourant, C., Bertout, C., & Benevides-Soares, P. 2012, A&A, 538, A23
Gottlieb, D. M., & Upson, W. L. 1969, ApJ, 157, 611
Guieu, S., Dougados, C., Monin, J.-L., Magnier, E., & Martín, E. L. 2006, A&A, 446, 485
Herbig, G. H. 1965, ApJ, 141, 588
Herbig, G. H. 1978, in Problems of Physics and Evolution of the Universe, ed. L. V. Mirzoyan (Yerevan: Armenian Academy of Sciences), 171
Jensen, E. L. N. 2001, in ASP Conf. Ser. 244, Young Stars Near Earth: Progress and Prospects, ed. R. Jayawardhana & T. Greene (San Francisco, CA: ASP), 3
Joncour, I., Duchêne, G., & Moraux, E. 2017, A&A, 599, A14
Jones, D. H. P. 1971, MNRAS, 152, 231
Kraus, A. L., Herczeg, G. J., Rizzuto, A. C., et al. 2017, ApJ, 838, 150
Kroupa, P. 2001, MNRAS, 322, 231
Lim, B., Sung, H., Kim, J. S., et al. 2016, ApJ, 831, 116
Luhman, K. L. 2004, ApJ, 617, 1216
Luhman, K. L. 2007, ApJS, 173, 104
Luhman, K. L. 2018, AJ, 156, 271
Luhman, K. L., Mamajek, E. E., Allen, P. R., & Cruz, K. L. 2009, ApJ, 703, 399
Luhman, K. L., Mamajek, E. E., Shukla, S. J., & Loutrel, N. P. 2017, AJ, 153, 46
Luo, A.-L., Zhang, H.-T., Zhao, Y.-H., et al. 2012, RAA, 12, 1243
Milne, D. K., & Aller, L. H. 1980, AJ, 85, 17
Murphy, S. J., & Lawson, W. A. 2015, MNRAS, 447, 1267

Oh, S., Price-Whelan, A. M., Hogg, D. W., Morton, T. D., & Spergel, D. N. 2017, AJ, 153, 257

Ortega, V. G., Jilinski, E., de la Reza, R., & Bazzanella, B. 2009, AJ, 137, 3922

Röser, S., Schilbach, E., Goldman, B., et al. 2018, A&A, 614, A81

Smart, W. M. 1968, Stellar Kinematics (London: Longmans)

Song, I., Zuckerman, B., & Bessell, M. S. 2003, ApJ, 599, 342

Stauffer, J. R. 1980, AJ, 85, 1341

Su, D.-Q., & Cui, X.-Q. 2004, ChJAA, 4, 1

Taylor, M. B. 2005, in ASP Conf. Ser. 347, Astronomical Data Analysis Software and Systems XIV, ed. P. Shopell, M. Britton, & R. Ebert (San Francisco, CA: ASP), 29

Tetzlaff, N., Neuhäuser, R., & Hohle, M. M. 2011, MNRAS, 410, 190

Tognelli, E., Degl'Innocenti, S., & Prada Moroni, P. G. 2012, A&A, 548, A41

Tonry, J. L., Stubbs, C. W., Lykke, K. R., et al. 2012, ApJ, 750, 99

Torres, G., Winn, J. N., & Holman, M. J. 2008, ApJ, 677, 1324

Walter, F. M. 1986, ApJ, 306, 573

Wang, S., & Chen, X. 2019, ApJ, 877, 116

Wang, S., Jiang, B. W., Zhao, H., et al. 2017, ApJ, 848, 106

Weymann, R., & Sears, R. L. 1965, ApJ, 142, 174

Wichmann, R., Bastian, U., Krautter, J., Jankovics, I., & Rucinski, S. M. 1998, MNRAS, 301, L39